Nanostructuring of Sensors Determines the Efficiency of Biomolecular Capture

ARTICLE *in* ANALYTICAL CHEMISTRY · JULY 2010

Impact Factor: 5.64 · DOI: 10.1021/ac101164n · Source: PubMed

3 AUTHORS, INCLUDING:

Edward H Sargent
University of Toronto
418 PUBLICATIONS **13,829** CITATIONS
SEE PROFILE

Shana O Kelley
University of Toronto
117 PUBLICATIONS **3,912** CITATIONS
SEE PROFILE

Anal. Chem. **2010,** *82,* 5928–5931

Letters to *Analytical Chemistry*

Nanostructuring of Sensors Determines the Efficiency of Biomolecular Capture

Xiaomin Bin,[†] Edward H. Sargent,[‡] and Shana O. Kelley*[,†,§]

Department of Pharmaceutical Sciences, Leslie Dan Faculty of Pharmacy, Department of Biochemistry, Faculty of Medicine, and Department of Electrical and Computer Engineering, Faculty of Engineering, University of Toronto, Toronto, Canada

The detection of biologically important molecules such as proteins and nucleic acids is of high and growing interest in the diagnosis of diseases from cancer to infectious and cardiovascular disease. The use of nanostructures to enhance sensitivity in biomolecular detection has now been reported in a broad range of assays. Here we provide direct evidence that the display of nucleic acid probe molecules on a nanostructured surface dramatically enhances hybridization efficiency compared to the case of the same probe molecules tethered on a smoother surface. Another factor expected to influence hybridization is the density of the probe monolayer. Remarkably, we find herein that the effect of nanostructuring dominates over probe density: the benefits of a high degree of nanostructuring can more than overcome the influence of dense probe packing. The results obtained herein give guidance to the development of high-performance biosensors for medical and environmental applications.

A wide range of nanoscaled materials such as nanowires,[1−8] nanotubes,[9−11] nanoparticles[12−15] and nanotextured surfaces[16−20] have been tested as biosensing devices. Many of these studies have indicated that nanostructures are highly beneficial for biosensing applications. However, there are few studies that provide detailed breakdown of the detection process into a series of identifiable steps and that are thus able to pinpoint the precise physical origins of any enhancement in sensitivity that is observed.

We recently reported the precise manipulatation of the surface morphology of sensors by controlling the level of nanostructuring present on a microscale electrode.[16−19] We refer to these as nanostructured microelectrodes (NMEs). NMEs provide a platform to systematically study the sensitivity as a function of the degree of nanostructuring on biosensing elements. In the prior work on these structures, we showed that they could be used as ultrasensitive biosensors and that limits of detection for nucleic acids analytes were intimately linked to the degree of nanostructuring present on a sensor surface. However, the origin of this link remained unexplained and poorly understood. Here, in this letter, we conduct detailed experiments exploring the complexation efficiencies for DNA strands binding with probe molecules immobilized on differently nanostructured sensors. The results reveal that the improved limits of detection realized with finely nanostructured sensors stem directly from the improved complexation efficiencies obtained.

In theory, two hypotheses could explain the nanostructuring−sensitivity connection: (1) nanostructured electrodes possess increased surface area, and the increase in capture sites or signal then promotes higher sensitivity and/or (2) the display of probes on a nanostructured electrode surface enhances accessibility during hybridization, leading to faster and more efficient binding

* To whom correspondence should be addressed. E-mail: shana.kelley@utoronto.ca.
† Department of Pharmaceutical Sciences, Leslie Dan Faculty of Pharmacy.
‡ Department of Electrical and Computer Engineering, Faculty of Engineering.
§ Department of Biochemistry, Faculty of Medicine.

(1) Hahm, J.-i.; Lieber, C. M. *Nano Lett.* **2003**, *4*, 51.
(2) Cui, Y.; Wei, Q.; Park, H.; Lieber, C. M. *Science* **2001**, *293*, 1289.
(3) Gao, X. P. A.; Zheng, G.; Lieber, C. M. *Nano Lett.* 2009.
(4) Stern, E.; Klemic, J. F.; Routenberg, D. A.; Wyrembak, P. N.; Turner-Evans, D. B.; Hamilton, A. D.; Lavan, D. A.; Fahmy, T. M.; Reed, M. A. *Nature* **2007**, *445*, 519.
(5) Roberts, M. A.; Kelley, S. O. *J. Am. Chem. Soc.* **2007**, *129*, 11356.
(6) Pampalakis, G.; Kelley, S. O. *Analyst* **2009**, *134*, 447.
(7) Fang, Z.; Kelley, S. O. *Anal. Chem.* **2008**, *81*, 612.
(8) Xiao, Y.; Patolsky, F.; Katz, E.; Hainfeld, J. F.; Willner, I. *Science* **2003**, *299*, 1877.
(9) Chen, R. J.; Bangsaruntip, S.; Drouvalakis, K. A.; Wong Shi Kam, N.; Shim, M.; Li, Y.; Kim, W.; Utz, P. J.; Dai, H. *Proc. Natl. Acad. Sci. U.S.A.* **2003**, *100*, 4984.
(10) Heller, I.; Janssens, A. M.; Mannik, J.; Minot, E. D.; Lemay, S. G.; Dekker, C. *Nano Lett.* **2007**, *8*, 591.
(11) Yu, X.; Munge, B.; Patel, V.; Jensen, G.; Bhirde, A.; Gong, J. D.; Kim, S. N.; Gillespie, J.; Gutkind, J. S.; Papadimitrakopoulos, F.; Rusling, J. F. *J. Am. Chem. Soc.* **2006**, *128*, 11199.
(12) Nam, J.-M.; Thaxton, C. S.; Mirkin, C. A. *Science* **2003**, *301*, 1884.
(13) Alivisatos, P. *Nat. Biotechnol.* **2004**, *22*, 47.
(14) Burda, C.; Chen, X.; Narayanan, R.; El-Sayed, M. A. *Chem. Rev.* **2005**, *105*, 1025.
(15) Mani, V.; Chikkaveeraiah, B. V.; Patel, V.; Gutkind, J. S.; Rusling, J. F. *ACS Nano* **2009**, *3*, 585.
(16) Taft, B. J.; Lazareck, A.; Xu, J. M.; Kelley, S. O. *J. Am. Chem. Soc.* **2004**, *126*, 12750.
(17) Yang, H.; Hui, A.; Pampalakis, G.; Soleymani, L.; Liu, F.-F.; Sargent, E. H.; Kelley, S. O. *Angew. Chem., Int. Ed.* **2009**, *48*, 8461.
(18) Soleymani, L.; Fang, Z.; Sun, X.; Yang, H.; Taft, B.; Sargent, E. H.; Kelley, S. O. *Angew. Chem., Int. Ed.* **2009**, *48*, 8457.
(19) Soleymani, L.; Fang, Z.; Sargent, E. H.; Kelley, S. O. *Nat. Nanotechnol.* **2009**, *4*, 844.
(20) Fang, Z.; Soleymani, L.; Pampalakis, G.; Yoshimoto, M.; Squire, J. A.; Sargent, E. H.; Kelley, S. O. *ACS Nano* **2009**, *3*, 3207.

10.1021/ac101164n
Published on Web 06/22/2010

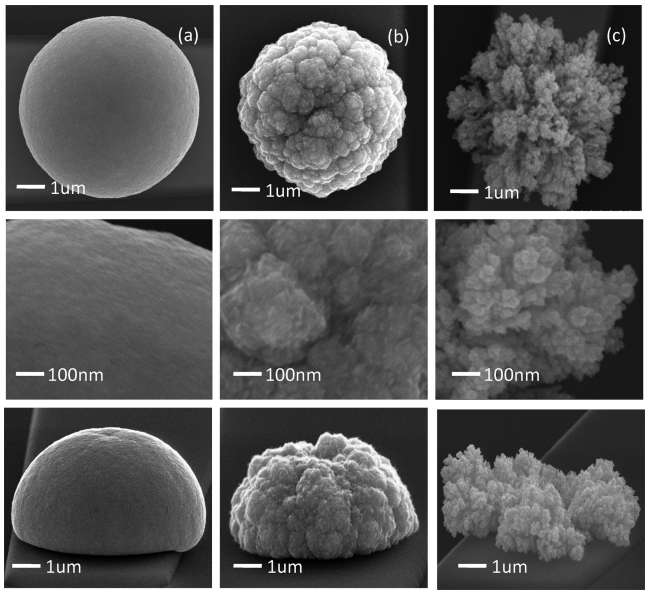

Figure 1. The scanning electron microscopy (SEM) images of three Pd NMEs fabricated with different levels of nanostructuring: (a) smooth surfaces, (b) moderately nanostructured surface with a feature size of 100−150 nanometers, and (c) finely nanostructured surface with a feature size of 20−30 nanometers. These structures were originally developed to analyze biosensing limits of detection as described in ref 19.

of analyte. In order to examine these two hypotheses, we sought to directly evaluate the probe surface coverage and target capture efficiency (i.e., hybridization efficiency) of three classes of NMEs. We were able to control both the degree of nanostructuring and also the surface area, allowing us to investigate each of the hypotheses above.

Three different types of palladium NMEs with different levels of nanostructuring were fabricated by electrodeposition on a microfabricated chip according to the procedure reported previously.[19] By controlling the deposition time, applied potential, metal ion concentration, and the composition of electrolyte, we are able to manipulate the size and surface morphology precisely. Figure 1 shows the scanning electron microscopy (SEM) images of three NMEs, including (a) a smooth hemispherical sensor, (b) a moderately nanotextured sensor with a feature size of 100−150 nm, and (c) a finely nanotextured sensor with a feature size of 20−30 nm.

The surface areas of Pd NMEs were evaluated by monitoring and integrating the Pd oxide reduction peak area of a cyclic voltammogram measured under acidic conditions. In each cycle, a monolayer of chemisorbed oxygen is formed and reduced, and the quantitation of this signal is used to calculate the active surface area. Using this technique, we determined the surface areas of the NMEs. The values were usually in the range $6-9\times10^{-5}$ cm^2. We then proceeded to use only structures with the same surface area in order to eliminate it as an experimental variable.

In order to assess differences in the densities of probe monolayers on the differently nanostructured NMEs, thiolated ssDNA was deposited on the sensors and surface coverage was determined using a chronocoulometric method based on that reported by Steel et al.[26] In the low ionic strength buffer, trivalent $Ru(NH_3)_6^{3+}$ preferentially exchanges with the native monovalent DNA counterions until they are essentially completely replaced, electrostatically associating to the singly negatively charged DNA phosphate groups in the ratio 1:3. The charge Q as a function of time t from the potential step is the sum of the reduction of $Ru(NH_3)_6^{3+}$ diffusing from solution, the double layer charge, and the charge due to reduction of surface confined $Ru(NH_3)_6^{3+}$ and is given by the integrated Cottrell equation:

$$Q = \frac{2nFAD_0^{1/2}C_0^*}{\pi^{1/2}}t^{1/2} + Q_{dl} + nFA\Gamma_0 \qquad (1)$$

where n is the number of electrons per molecule for reduction, F the Faraday constant (coulomb/mole), A the electrode area (centimeters squared), D_0 the diffusion coefficient (centimeters squared/second), C_0^* the bulk concentration of $Ru(NH_3)_6^{3+}$ (moles/centimeters cubed), Q_{dl} the capacitive charge (coulombs), and $nFA\Gamma_0$ the charge from the reduction of Γ_0, the amount of surface confined redox marker (moles/centimeters squared). Chronocoulometric data is plotted as an Anson plot of Q versus $t^{1/2}$. Extrapolation of a least-squares fit to the linear part was used to determine the intercept at time zero, which corresponds to $Q_{dl} + nFA\Gamma_0$. Assuming the double layer capacitance to be approximately equal in measurements with and without $Ru(NH_3)_6^{3+}$, Q_{dl} for the fixed voltage step is constant and $nFA\Gamma_0$ is calculated as the difference in intercepts. The DNA surface coverage is determined from the surface excess of $Ru(NH_3)_6^{3+}$ as

$$\Gamma_{DNA} = \Gamma_0\left(\frac{z}{m}\right)N_A \qquad (2)$$

where Γ_{DNA} is the probe surface coverage (molecules/centimeters squared), m is the number of phosphate groups on the probe DNA, z is the charge on the redox molecule, and N_A is Avogadro's number.

Typical chronocoulometric response curves for a DNA modified Pd NME in the absence and presence of $Ru(NH_3)_6^{3+}$ are shown in Figure 2. Because of the short time scale of these experiments (100 ms), the measurements report on diffusion-controlled signals, whereas a longer collection time will result in the loss of linearity of the Q versus $t^{1/2}$ curve, since it reaches steady state. As a control, chronocoulometry for pure mercaptohexanol (MCH)-modified NMEs were examined in the presence and absence of $Ru(NH_3)_6^{3+}$ to confirm that the same intercept was obtained from a linear fit of Q as a function of $t^{1/2}$ (Figure S1 in the Supporting Information). This indicates that the Γ_0 values obtained from chronocoulometric measurements of ssDNA modified NMEs are from $Ru(NH_3)_6^{3+}$ associated with negatively charged DNA. Moreover, it was observed that values of Q_{dl} in buffer solutions varied before and after hybridization, and thus careful calibration and correction of these values was done as described in the Supporting Information.

The surface coverage of ssDNA on three different Pd NMEs was determined as shown in Figure 3. The surface coverage of finely nanostructured NMEs is $9 \pm 1 \times 10^{12}$ molecules/cm^2, which is higher than that of moderately nanostructured or smooth NMEs ($5 \pm 1 \times 10^{12}$ and $6 \pm 2 \times 10^{12}$) molecules/cm^2,

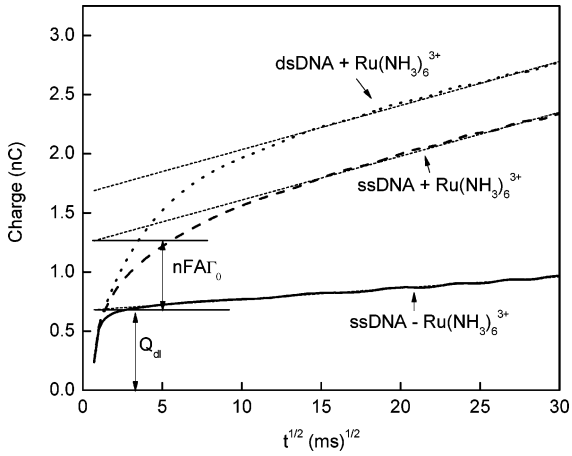

Figure 2. Typical chronocoulometric response curves for DNA modified Pd NMEs. --- is the least-squares fit to the linear region. Chronocoulometry traces were recorded in the presence and absence of $Ru(NH_3)_6^{3+}$ before and after hybridization to (i) quantitate the background double-layer charging (Q_{dl}) and measure the charge derived from the DNA-associated Ru(III) that is a measurement of DNA surface coverage. See the Supporting Information for information on the variation of Q_{dl} as a function of hybridization.

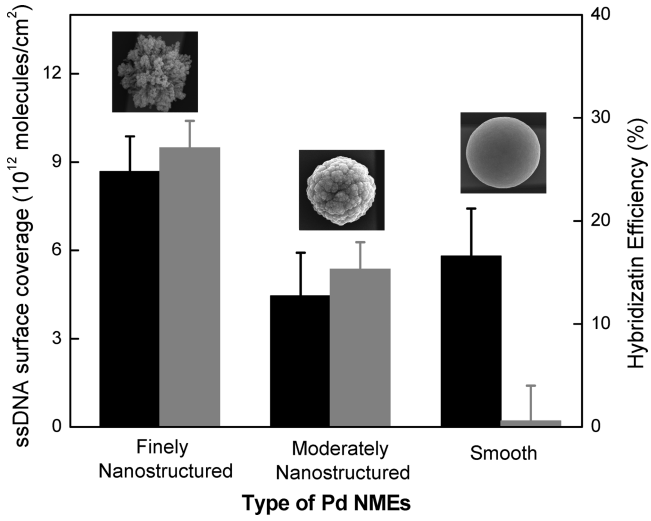

Figure 3. Surface coverage of ssDNA modified Pd NMEs (black bars) and their hybridization efficiencies to target DNA (gray bars).

respectively. Over 30 separate electrodes for each type of NMEs were used to generate the statistically meaningful results with error values. Clearly, more probe molecules can be adsorbed onto a finely nanostructured surface. While we cannot prove that the coverage of probes is uniform on the sensor surfaces, the fact that the density of probe molecules closely matches what has been observed in other materials systems,[27] it is likely that probe is immobilized on most areas of the working area of the sensor.

To assess the target capture efficiency, ssDNA modified Pd NMEs were incubated with a complementary sequence of target DNA. Hybridization efficiency (HE) can be obtained as follows:

$$\mathrm{HE}\% = \frac{\Gamma_{\mathrm{dsDNA}} - \Gamma_{\mathrm{ssDNA}}}{\Gamma_{\mathrm{ssDNA}}} \times 100\% \qquad (3)$$

Table 1. Average Values for Surface Coverage, Feature Size, and Calculated Deflection Angles

Pd NMEs	coverage ($\times 10^{12}$) (molecules/cm^2)	feature size (nm)	deflection angle (deg)
finely nanostructured	8.7 ± 1.2	25	18 ± 6
moderately nanostructured	4.5 ± 1.4	150	4.1 ± 2.0
smooth	5.8 ± 1.6	1000 or larger	0.5 ± 0.2 or smaller

where Γ_{ssDNA} and Γ_{dsDNA} are surface coverage before and after hybridization.

The hybridization efficiency of these three DNA modified Pd NMEs revealed a very interesting trend. As shown in Figure 3, the highly nanostructured NME, even with high surface coverage of ssDNA ($\sim 9 \times 10^{12}$ molecules/cm^2), exhibited the highest hybridization efficiency, contrary to literature results that higher surface density of ssDNA (usually larger than 4×10^{12} molecules/cm^2) will lead to lower hybridization efficiency.[22−26] More moderately nanostructured NMEs showed lowered hybridization efficiencies, and smooth NMEs without any nanoscale features show even lower hybridization efficiencies. Given that the surface area was normalized in these experiments, these studies clearly point toward the validation of a hypothesis focused on the influence of nanoscale morphology on probe display and accessibility.

The results described provide direct evidence that the size of the nanostructures present on a sensor surface influences the probe density and facilitates nucleic acid hybridization. Recent studies of the effect of the radius of the curvature of nanoparticles on the surface density of DNA[27] provides a useful model to describe how the radius of the curvature of nanostructures affects the interaction between neighboring oligonucleotide strands. A smaller radius of curvature was proposed to provide a larger deflection angle between probes and thereby promote higher surface coverage. Table 1 showed calculated interprobe deflection angles for the three types of Pd NMEs. The deflection angle appears to influence the NME system as well, with higher probe densities observed on the sensors with the smallest nanostructures. In the present report, we are, in addition to being able to evaluate surface coverage, also able to quantitate hybridization efficiency. Our finding that higher levels of nanostructure enhance hybridization efficiency suggests that larger deflection angles may also be responsible for allowing target molecules better access to complementary probes. This hypothesis is summarized in Figure 4.

While the model presented - linking probe density and accessibility on highly nanostructured sensors with higher hybridization efficiency - appears to adequately explain the trends

(21) Demers, L. M.; Mirkin, C. A.; Mucic, R. C.; Reynolds, R. A.; Letsinger, R. L.; Elghanian, R.; Viswanadham, G. *Anal. Chem.* **2000**, *72*, 5535.
(22) Peterson, A. W.; Heaton, R. J.; Georgiadis, R. M. *Nucleic Acids Res.* **2001**, *29*, 5163.
(23) Lapierre, M. A.; O'Keefe, M. M.; Taft, B. J.; Kelley, S. O. *Anal. Chem.* **2003**, *75*, 6327.
(24) Keighley, S. D.; Li, P.; Estrela, P.; Migliorato, P. *Biosens. Bioelectron.* **2008**, *23*, 1291.
(25) Ricci, F.; Lai, R. Y.; Heeger, A. J.; Plaxco, K. W.; Sumner, J. J. *Langmuir* **2007**, *23*, 6827.
(26) Steel, A. B.; Herne, T. M.; Tarlov, M. J. *Anal. Chem.* **1998**, *70*, 4670.
(27) Hill, H. D.; Millstone, J. E.; Banholzer, M. J.; Mirkin, C. A. *ACS Nano* **2009**, *3*, 418.

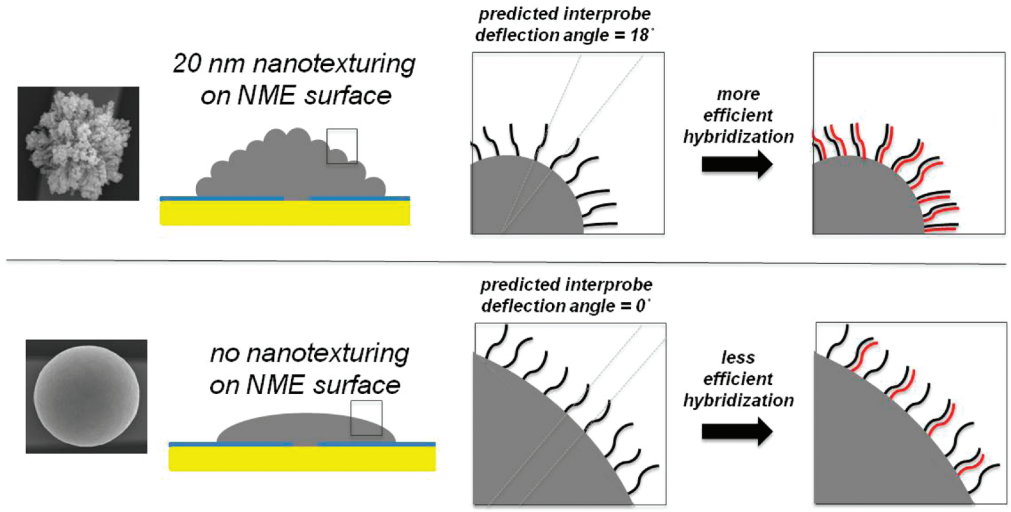

Figure 4. Proposed model of the effect of nanostructuring on surface loading of DNA molecules and their hybridization.

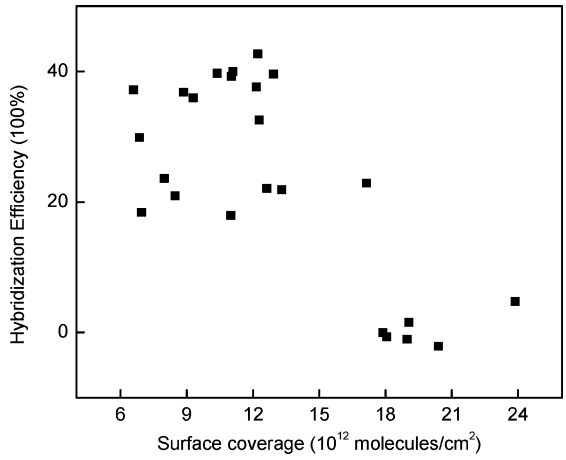

Figure 5. Hybridization efficiency as a function of ssDNA surface coverage on the finely nanostructured Pd NME surfaces.

observed, the fact that higher surface coverage is observed might also contribute. For example, having more probe molecules on a sensor could allow adjacent probe molecules to replace poorly formed complexes without allowing target escape, keeping targets at the sensor surface more effectively. We therefore tested even higher surface coverages of DNA on our most nanostructured sensors. With variation of the probe deposition time and the ionic strength of the ssDNA probe deposition solution, we were able to vary the probe density as shown in Figure 5. We examined a variety of sensors with differing surface coverages and could see a clear trend toward diminshed hybridization efficiency at higher surface coverages. This indicates that the accessibility and display of probes is a more important factor than any benefits from high probe density in promoting efficient target capture.

In summary, we systematically investigated the impact of nanostructuring on the capture of biomolecular targets. The surface coverage and hybridization efficiency of three different Pd microelectrodes with different levels of nanostructuring were measured by an electrochemical chronocoulometric method. The results showed that the hybridization efficiency of ssDNA probes to their target is higher when the feature size of the nanostructure of the electrode surface is smaller. This work provides direct evidence for nanostructure-facilitated nucleic acids hybridization. It elucidates that surface morphology may play an important role in any interfacial biomolecular probe-target interaction, such as nucleic acid hybridization, antigen−antibody interactions, etc. The recent observation of enhanced binding of circulating tumor cells to nanostructured surfaces may be linked to effect described.[28] Thus, the observations reported here may guide the development of both sensors and other materials used for biocapture.

ACKNOWLEDGMENT

We wish to acknowledge Genome Canada/Ontario Genomics Institute, the Ontario Ministry of Innovation and Research, the Ontario Centres of Excellence, Ontario Institute for Cancer Research, Canada Foundation for Innovation, Canadian Institutes of Health Research, and NSERC for their support of this work.

SUPPORTING INFORMATION AVAILABLE

Additional information as noted in text. This material is available free of charge via the Internet at http://pubs.acs.org.

Received for review May 4, 2010. Accepted May 4, 2010.

AC101164N

(28) Wang, S.; Wang, H.; Jiao, J.; Chen, K.-J.; Owens, Gwen E.; Kamei, K.-i.; Sun, J.; Sherman, D. J.; Behrenbruch, C. P.; Wu, H.; Tseng, H. R. *Angew. Chem., Int. Ed.* **2009**, *48*, 8970.